Vol. 140: 227–237, 1996 | MARINE ECOLOGY PROGRESS SERIES
Mar Ecol Prog Ser | Published September 12

Impact of biogenic sediment topography on oxygen fluxes in permeable seabeds

Wiebke Ziebis*, Markus Huettel, Stefan Forster

Max Planck Institute for Marine Microbiology, Celsiusstr. 1, D-28359 Bremen, Germany

ABSTRACT: Boundary layer flows, interacting with roughness elements at the sediment surface, alter the small-scale flow regime. Consequently, pressure differences are generated that are the driving forces for advective pore-water flow. We investigated topography-induced transport of oxygen in a permeable coastal sediment from the Mediterranean Sea (Isola del Giglio, Italy). The sediment surface was characterized by a high abundance (120 m^{-2}) of sediment mounds (average height: 4 cm) built by the mud shrimp *Callianassa truncata* (Decapoda, Thalassinidea). Boundary layer flow velocities recorded *in situ* ranged between 2 and 16 cm s^{-1}. Detailed experiments were performed in a recirculating laboratory flow channel. A natural sediment core, 20 cm deep with a surface area of 0.3 m^2, was exposed to a unidirectional flow of varying current velocity (3, 6, 10 cm s^{-1}). The alteration of the small-scale flow regime at a sediment mound was documented by vertical velocity profiles measured in 1 mm resolution with temperature-compensated thermistor probes. Oxygen distribution in the sediment was investigated with Clark-type microelectrodes. At a smooth surface, oxygen penetration depth in the permeable sediment did not exceed 4 mm, independent of flow velocity. In contrast, the topography-induced advective oxygen transport increased significantly with current speed. Oxygen reached down to almost 40 mm at the upstream foot of a 1 cm high sediment mound at a flow velocity of 10 cm s^{-1}. Thus, the oxic sediment volume increased locally by a factor of 4.8 compared to the oxic zone underneath a smooth surface. At a natural abundance of 120 mounds m^{-2} the oxic sediment volume per m^2 seabed was calculated to be 3.3-fold higher than in a seabed with a smooth surface. In a parallel experiment, advective solute transport was also demonstrated in a less permeable sediment ($k = 5 \times 10^{-12}$ m^2) from the North Sea intertidal flat. Due to the lower permeability the effect on O_2 transport was less than in the Mediterranean sand, but oxygen penetration depth increased locally 2-fold at a sediment mound under a flow velocity of 10 cm s^{-1}. The experiments showed the high spatial and temporal variability of oxygen distribution in a coastal seabed depending on sediment surface topography, boundary layer flow velocities and sediment permeability.

KEY WORDS: Oxygen · Advective transport · Boundary layer flow · Permeable sediment · *Callianassa truncata* · Sediment-water exchange

INTRODUCTION

Among the chemical species being transferred between the water column and the sediment, oxygen plays a key role in biological and geochemical processes. The supply of oxygen to the seabed is essential for aerobic life within the sediment. Among the electron acceptors in marine sediments, oxygen is energetically the most valuable for the mineralisation of organic compounds and the chemical or bacterial oxidation of reduced products from anaerobic mineralisation. It also affects the availability of respiratory electron acceptors within the sediment column used in anaerobic microbial processes. Nitrate and sulphate for example are regenerated from ammonia and sulphide through oxidation by O_2. The extent of the oxic (containing oxygen) and oxidised zone (having positive redox potential) regulates the distribution of bacterial and protozoan communities (Fenchel 1969, Blackburn 1987, Giere 1993, Berninger & Epstein 1995, Fenchel & Finlay 1995). In turn, the zonation of microbial activity has a strong influence on organic matter degradation, mineral cycling and nutrient

*E-mail: wiebke@postgate.mpi-mm.uni-bremen.de

release from the sediment (Fenchel & Blackburn 1979, Meyer-Reil et al. 1987, Mackin & Swider 1989, Jørgensen & Revsbech 1989).

In situ investigations revealed that in coastal environments oxygen penetrates by diffusion from the overlying water usually not deeper than 2 to 5 mm into the sediment (Revsbech et al. 1980, Andersen & Helder 1987). Burrowing macrofauna transport supernatant water to deeper sediment layers by irrigating their tubes and burrows. Dissolved substances, like oxygen, diffuse through the burrow walls (Aller 1983, Forster & Graf 1992) into the ambient sediment. The enlargement of the sediment-water interface can considerably increase the solute exchange between the seabed and the overlying water (Hylleberg & Henriksen 1980, Aller 1982, Kristensen 1985, Huettel 1990) depending on the density of organisms and their bioturbation and bioirrigation behaviour (Forster & Graf 1995).

In areas exposed to tidal waves and strong bottom currents, hydrodynamic forces can resuspend and thereby oxygenate surficial sediment or flush the interstices with oxygen-rich water (Riedl et al. 1972, Malan & McLachlan 1991).

Coastal environments are characterised by biogenic structures (mounds, pits, tracks and funnels) created by infaunal and epifaunal organisms and by geological features (ripples) in a variety of morphologies and sizes. These structures strongly affect the small-scale flow regime at the interface, as flow velocity is locally increased or decreased (Vogel 1983, Schlichting 1987, Yager et al. 1993). The velocity gradients generate pressure differences that constitute driving forces for an advective solute transport across the interface of permeable seabeds (Thibodeaux & Boyle 1987, Huettel & Gust 1992). Thus, the topography of the sea-floor can be of importance for the interfacial solute exchange in coastal sediments.

We investigated the role of advective oxygen transport at the sediment surface caused by the interaction of biogenic sediment topography with boundary layer flows. We investigated the distribution of oxygen with polarographic microelectrodes in a natural sediment core characterised by biogenic mounds created by the mud shrimp *Callianassa truncata* (Decapoda, Thalassinidea). Our results show that advective oxygenation effects can reach several centimetres sediment depth, depending on the surface topography, the flow velocity of bottom currents and the sediment permeability.

MATERIALS AND METHODS

Study site and origin of sediments. The sediment core for the laboratory flume experiments originated from the Bay of Campese at the west coast of Giglio Island in the Mediterranean Sea (Fig. 1). As part of the Tuscany Archipelago, the island is situated ca 150 km northwest of Rome (42° 20' N, 10° 52' E) off the west coast of Italy and has an area of 21 km^2 with 28 km coastline. The sediment surface in the shallow bay is characterised by conspicuous mounds created by the mud shrimp *Callianassa truncata* (Decapoda, Thalassinidea) (Fig. 2). Thalassinids are burrowing crustaceans that are common and often abundant in soft sediments of temperate and tropical coastal environments (Dworschak 1983, Griffis & Suchanek 1991). While constructing and maintaining its burrow, *C. truncata* ejects excavated sediment in a fountain-like manner through a burrow opening at the sediment surface, forming volcano-shaped mounds with an average height of 4 cm (maximum 9 cm). These biogenic features are abundant throughout the shallow part of the bay (2 to 25 m water depth) and cover the sediment surface in an average density of 120 ± 43 mounds m^{-2} (n = 240) (Ziebis unpubl.). The mounds are rebuilt within 1 to 2 h if erased by wave action when storms occasionally occur. Prevailing regional currents passing the island in a south-north direction generate a clockwise gyre within the bay (Fig. 1). From May to August predominant wind directions are NW and W, with 70% of the recorded wind speeds being in the range of 1 to 3 on the Beaufort scale (ca 0.3 to 5.4 m s^{-1}). The bay is sheltered from southerly strong winds prevailing in late autumn, winter and early spring. Boundary flow velocities and directions were measured from May to August

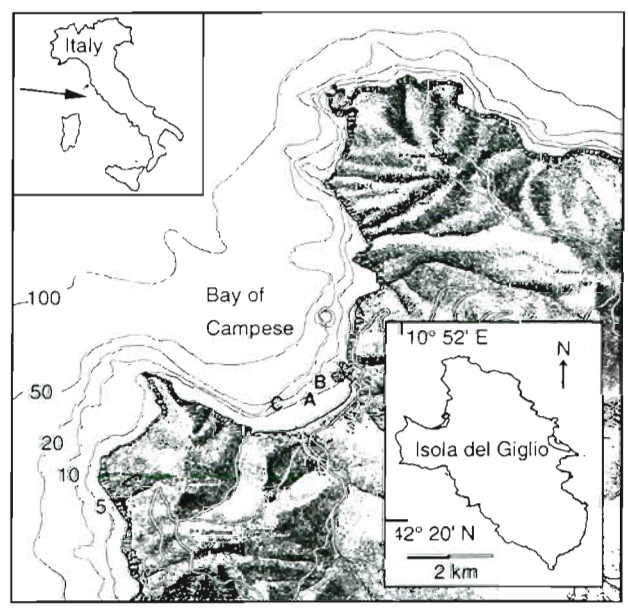

Fig. 1. Giglio Island, Tyrrhenian Sea. The study site and sampling area was in the Bay of Campese on the west coast of the island. Sites A, B, and C were in 5, 7 and 12 m water depth respectively

using a mechanical current-meter (Mini Air-Water 2, Schiltknecht) connected to a tripod which was lowered onto the sediment surface at Stns A to C (Fig. 1) at 5, 7, and 12 m water depths. At each water depth the flow velocity was recorded 5 cm above the sediment surface for periods of 12 h and recorded by a 12 bit data-logger in intervals of 2 s. Flow velocities ranged between 2 and 16 cm s^{-1} with an average current speed of 8.4 cm s^{-1}. The flow changed little in direction (max. 45°) and intensity during each deployment.

Sediment characteristics. Analyses of grain size composition within the upper sediment layer of 10 cm showed that the sediment throughout the shallow part of the bay (2 to 15 m water depth) was well sorted, 70 to 95% dry weight consisted of medium sand (200 to 630 µm). Sediment cores for the experimental set-up were recovered at Site A (Fig. 1) at 5 m depth using acrylic cylinders of 20 cm diameter pushed 30 cm into the sediment. At the same site, samples for the analyses of sediment parameters were taken. The median grain size (MD) was 350 µm, the average porosity (water content) was 0.4 ± 0.08 (n = 5) and organic content was 0.8% of dry weight (loss upon ignition at 540°C for 12 h). Permeability (k, numerical constant related to the pore space of a sediment) was determined with a constant head permeameter (Means & Parcher 1964) to be 5.1×10^{-11} m^2.

Shrimps were collected separately because within their deep burrows they are hardly caught by conventional sampling methods.

To investigate the impact of sediment permeability on interfacial exchange processes we used less-permeable North Sea sediment originating from an intertidal flat (Sahlenburg, Germany) for a parallel experimental set-up. The sediment consisted of muddy sand, had a median grain size of 200 µm and an average porosity of 0.38 ± 0.02 (n = 5). The organic content was 1.2% of dry weight. The permeability ($k = 5.4 \times 10^{-12}$ m^2) was 1 order of magnitude lower than that determined for the Mediterranean sediment.

Experimental set-up. Two identical recirculating laboratory flow channels similar to the one described by Vogel (1983) were used to simulate *in situ* conditions. The open, acrylic channel of the flume was 200 cm long, 30 cm wide and 12 cm deep. The drop box (60 cm long, 30 cm wide and 20 cm deep) holding a sediment core with a surface area of 0.3 m^2 exposed to flow was located 90 cm downstream. The sediment recovered from the 2 study sites was filled into the boxes and the remaining channel floor was covered 1 cm high with natural sediment flush with the core surface. Flow was produced by a rotating propeller situated in the return conduit. Flow velocity was controlled by a mechanical flow-meter (Mini Air-Water 2, Schiltknecht) located 5 cm above the sediment. The flow speed was regulated by adjusting the voltage of the electric motor. The recirculating water was kept at a constant temperature of 19°C by means of a cooling coil in the return conduit. Each flume contained 160 l of sea water, which had been transported from the sampling sites. The salinity was 37‰ for the Mediterranean set-up and 35‰ for the North Sea system.

Prior to the experiments, the sediment in both systems was allowed to equilibrate for 6 wk at a flow velocity of 10 cm s^{-1}. Before and between experiments, the channels were protected against light and the overlying water was aerated to keep the oxygen saturation at 97% air saturation.

The Mediterranean sediment core contained 7 individuals of *Callianassa truncata* that constructed 7 mounds (22 mounds m^{-2}) which were maintained throughout the experiment. We chose a mound situated on the centre line and 110 cm downstream for the measurements to avoid side wall effects.

Because in the North Sea core a biologically produced topography similar to the Mediterranean sediment was lacking, an artificial sediment mound of similar dimensions was built by hand on the centre line 110 cm downstream.

Small-scale flow velocity profiles. These were measured using temperature-compensated thermistor probes (LaBarbera & Vogel 1976) with a tip diameter of 0.8 mm and a 12 cm long slanted shaft with a maximum diameter of 1.2 mm. The flow sensors had a response time of 0.1 s. For the vertical profiles of flow velocity, the probes were moved by a micro-manipulator from the water column towards the sediment-water interface. Ten velocity profiles were measured in the Mediterranean set-up along the centre line of the flume starting 4 cm upstream of the *Callianassa truncata* mound and continuing in the direction of flow. Starting at 20 mm height above the sediment surface the flow velocities were measured in 1 mm intervals. For each step the data was recorded for 30 s. The free flow velocity 5 cm above the sediment surface was 6.5 cm s^{-1}.

Oxygen profiles. These were measured using Clark-type oxygen microelectrodes with a built-in reference and a guard cathode (Revsbech 1989). They had a tip diameter of 10 µm, a 90% response time of 1 s and showed no stirring sensitivity. Signals were amplified by a picoammeter and recorded on a strip-chart recorder or by a 12 bit data-logger. There was no drift in signal during the measurements. The electrodes were calibrated in air-saturated sea water of known oxygen concentration (Winkler titration) and in N_2-purged, oxygen-free sea water. The sensors were moved along x, y and z axes by a micro-manipulator. Vertical profiles were measured in intervals of typically 100 to 250 µm. The position of the sediment-water interface was determined visually through a dissecting

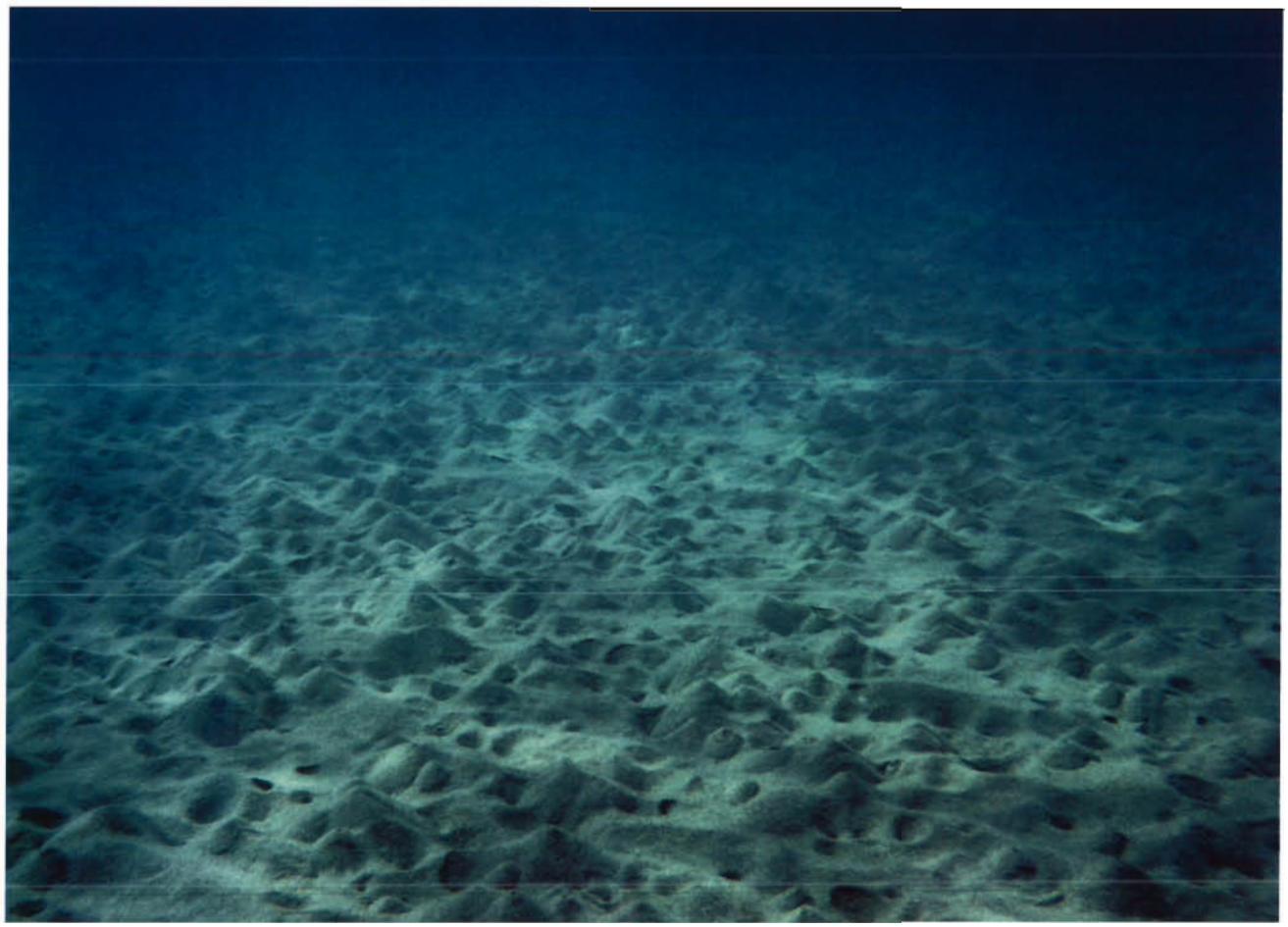

Fig. 2. Sediment surface topography at 5 m water depth in the Bay of Campese. The mounds are built by the mud shrimp *Callianassa truncata*. Mounds had an average height of 4 cm (max. 9 cm) and covered the sediment surface in an average density of 120 mounds m^{-2}

microscope as the first contact of the electrode with the sediment surface. The precision of surface detection was in the range of 1 sand grain (±350 µm Giglio sediment; ±200 µm North Sea sediment).

At a constant current speed of 10 cm s^{-1}, 8 profiles of oxygen concentration were measured in an area with a smooth surface in the Mediterranean core, to determine the penetration depth of oxygen in the absence of biotopography.

To assess the effect of topography on oxygen penetration depth, 14 oxygen profiles were measured along a transect starting 10 cm upstream of the 1 cm high mound to 10 cm downstream. At 4 positions, 2 upstream and 2 downstream, oxygen profiles along lines perpendicular to the main transect were measured, in order to document the lateral extension of oxygen intrusion.

To estimate the influence of boundary layer flow velocity on advective solute transport in a permeable seabed with biogenic surface topography, the same series of 14 oxygen profiles along the centre line was measured at flow velocities of 3 and 6 cm s^{-1} After a change in velocity the sediment was left for 12 h to equilibrate.

Parallel measurements were carried out in the North Sea sediment to assess the impact of sediment permeability on solute exchange across the sediment-water interface. Three series of 14 oxygen profiles were measured at current speeds of 3, 6 and 10 cm s^{-1} along a transect cross-sectioning the artificial mound.

RESULTS

Small-scale flow regime at a mound

Fig. 3 shows the flow velocity profiles of the unidirectional flow, as it passed over a 1 cm high *Callianassa truncata* mound. Mean values of the flow velocity recordings for periods of 30 s in 1 mm intervals were

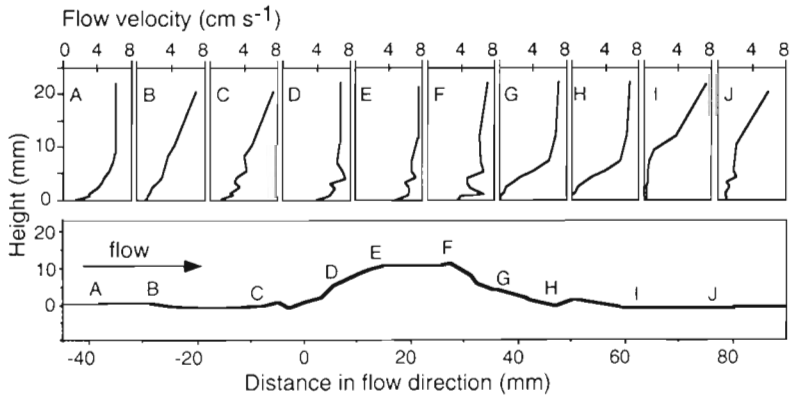

Fig. 3. Velocity profiles at a 1 cm high *Callianassa truncata* mound were measured in a laboratory flow channel. The lower graph shows the cross-section of the mound, which was situated on the centre-line of the channel. A to J indicate the positions of the measured flow profiles. Current velocity was measured in 1 mm intervals using a thermistor probe. Free flow velocity was 6.4 cm s^{-1}. Standard deviations for the measurements at positions A, B and G to J ranged between 0.05 and 0.2 cm s^{-1}, whereas at positions C to F, standard deviations below 10 mm water height were 0.25 to 0.35 cm s^{-1}, reflecting a more turbulent water flow

used to draw each profile. At 4 cm upstream of the mound (position A) the flow was undisturbed and the velocity profile was characterised by an increase of flow speed as the logarithm of the distance from the sediment surface. Closer to the mound (B, C) flow decreased in velocity below 10 mm height above the sediment surface, the same height as the roughness element. As the flow passed over the mound (D, E, F) it accelerated according to the principle of continuity and turbulent fluctuations close to the interface occurred. The maximum disturbance and flow separation were observed at the downstream edge of the mound (position F). At the downstream slope, flow slowed down, low velocities ($U < 4$ cm s^{-1}) were measured up to 5 mm above the sediment-water interface (positions G and H). There was an almost stagnant condition at the lee-side of the mound (position I). Due to these velocity gradients, pressure differences built up, with a low pressure area above the mound and high pressure areas upstream and downstream of the mound.

Effect of biogenic topography on oxygen transport

At a smooth sediment surface the average oxygen penetration under a current with a velocity of 10 cm s^{-1} was 3.6 ± 0.57 mm (n = 8). Six of the measured profiles are shown in Fig. 4. However, close to the mound the oxygen penetration changed in relation to the distance to the roughness element (Fig. 5). At 60 mm upstream of the mound, the steep decline of oxygen was similar to the smooth-surface profiles and the penetration depth of 6 mm was only slightly deeper. Starting at 50 mm upstream of the mound, oxygen penetrated deeper and the shape of the profiles changed. The gradients measured at the positions 10 mm in front ($x = -10$), at the foot ($x = 0$) and at the slope of the mound ($x = +10$) showed oxygen penetration depths of up to 36 mm, with high values continuing from the overlying water into the sediment. In 20 mm sediment depth there were still concentrations of 120 to 150 µmol oxygen l^{-1}. The topography-induced oxygen distribution is illustrated in Fig. 6. In the high pressure areas up- and downstream of the mound, overflowing water was forced into the sediment and the pore space was flushed with oxygen-rich water. In the downstream area the flushing effect was less intensive, but oxygen still reached down to 17 mm sediment depth. In the low pressure area, on top of the mound, anoxic pore-water from deeper layers was transported upward. Consequently a minimum of oxygen penetration was measured at the downstream edge.

We estimated the total oxic volume adjacent to the mound from the oxygen profiles measured along the main transect and along the 4 transects, perpendicular to it (positions: −30, −10, 60 and 75 mm), in the high pressure areas up- and downstream of the mound.

Assuming a 3-dimensional geometry of an elliptical half-sphere, volume (V) = $(4/3\ \pi\ a\ b\ c)/2$ (with a, b, and c being the half axes of an ellipsoid; a as the lateral extension, b as the distance along the centre line and c

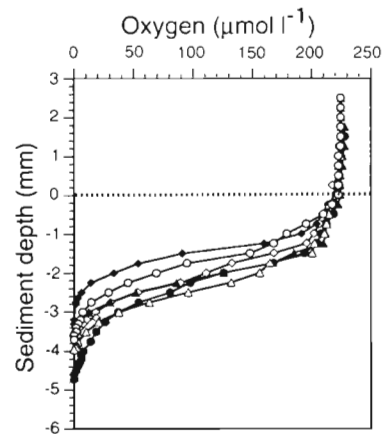

Fig. 4. At a smooth surface, at 8 positions along the centre line of the flume, oxygen profiles were measured under a current velocity of 10 cm s^{-1}. Six profiles are shown here. Average penetration depth of oxygen was 3.6 ± 0.57 mm (n = 8)

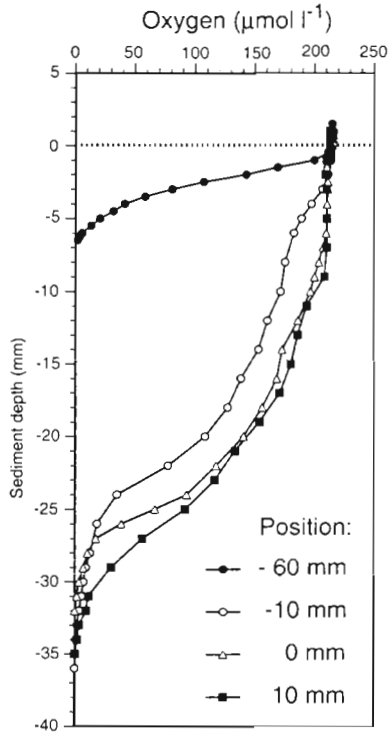

Fig. 5. Fourteen oxygen profiles were measured along a transect, cross-sectioning the mound (shown in Fig. 3) in flow direction, under a current velocity of 10 cm s^{-1}. Four selected profiles are shown here. Positions are given as distances in mm, where $x = 0$ is the position at the upstream foot of the mound. Negative values are further upstream, positive values are further downstream

as the maximum penetration depth), the oxic sediment volumes were estimated as V_1 = (4/3 π × 30 mm × 37.5 mm × 34 mm)/2 = 80 cm^3 upstream and V_2 = (4/3 π × 20 mm × 25 mm × 17 mm)/2 = 18 cm^3 downstream of the mound.

Effect of varying flow and sediment permeability

In the sandy Mediterranean sediment the penetration of oxygen in an area with a smooth sediment surface showed very little variation with flow velocity (Fig. 7). The penetration depth ranged from 4.3 mm at a current speed of 3 cm s^{-1} to 4.5 and 3.9 mm at current speeds of 6 and 10 cm s^{-1} respectively. Considering an accuracy of ±0.35 mm of surface determination (grain size: 350 µm), there was no significant increase of oxygen with current speed. The penetration depth of oxygen under stagnant conditions varied between 3 and 8 mm with a mean value of 4.8 mm (n = 6).

In contrast, the topography-induced solute transport varied essentially with flow velocity (Fig. 8). The maximum oxygen penetration measured at the same position ($x = 0$) in the high pressure area upstream of the mound ranged from 10 mm at 3 cm s^{-1} to 22 mm at 6 cm s^{-1} and reached 31 mm at 10 cm s^{-1}. Consequently the sediment volume supplied with oxygen was also clearly increasing with flow speed.

In the North Sea sediment, which consisted of less permeable, muddy sand, the penetration depth at a smooth surface under a flow of 10 cm s^{-1} was 4 ± 0.65 mm (n = 8). At the sediment mound there was no apparent effect on solute transport at current speeds of 3 and 6 cm s^{-1} (Fig. 9). Only at a flow velocity of 10 cm s^{-1} was a 2-fold increase in penetration depth of oxygen recorded in the high pressure area, upstream of the structure. There was no obvious effect on oxygen penetration in the area downstream of the mound. With a height of 8 mm, the artificial mound was slightly lower than the mounds built by *Callianassa truncata* in the Giglio sediment.

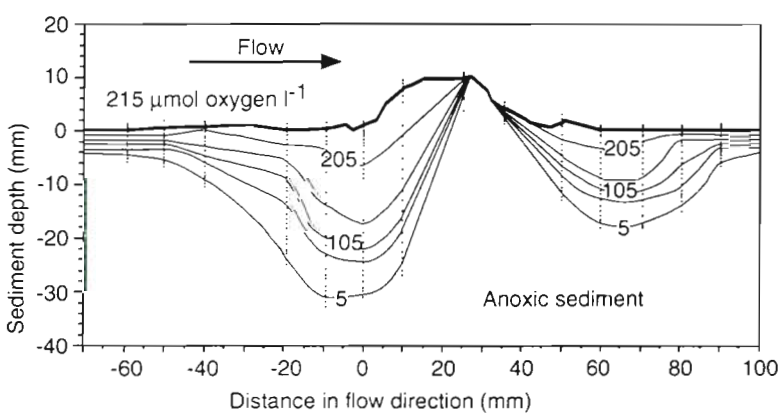

Fig. 6. Points of equal oxygen concentration were connected to illustrate the oxygen distribution underneath the sediment mound exposed to a flow velocity of 10 cm s^{-1}. Isopleths are shown in 50 µM intervals. Vertical dotted lines indicate the 14 measured oxygen profiles

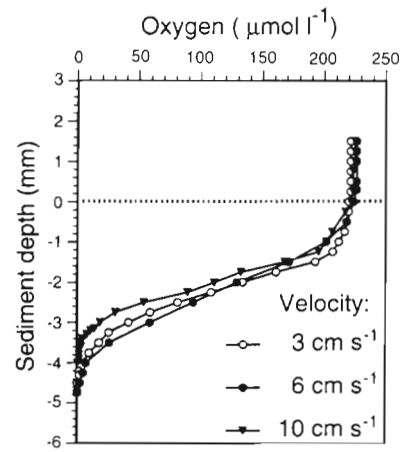

Fig. 7. At a smooth surface, oxygen profiles were measured at the same position, under 3 different flow velocities

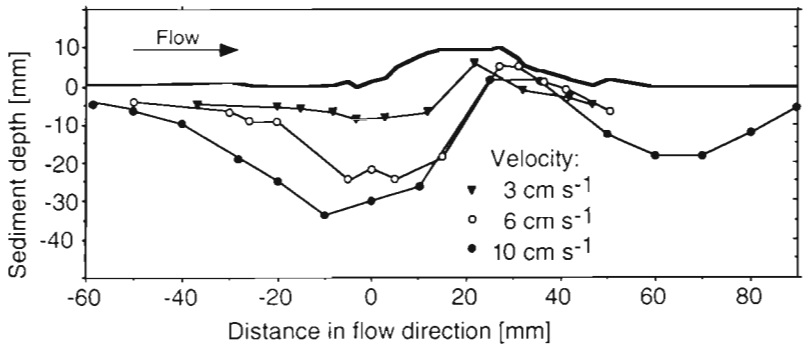

Fig. 8. Data points of the maximum oxygen penetration depths at the *Callianassa truncata* mound were connected (solid lines) to illustrate the oxygen penetration and distribution under 3 different flow velocities

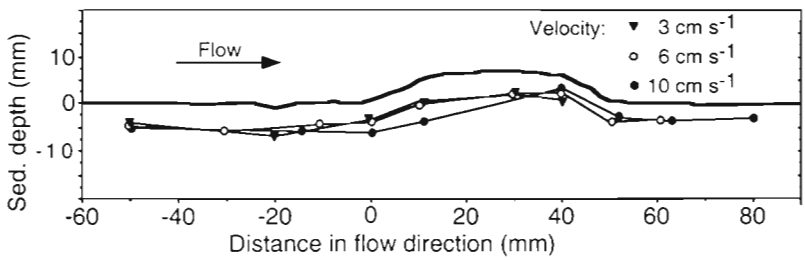

Fig. 9. Maximum oxygen penetration depths near a North Sea sediment mound, measured in a parallel set-up, are illustrated as solid lines for the 3 different current velocities. The North Sea sediment was less permeable ($k = 5.1 \times 10^{-12}$ m^2) than the Giglio sand ($k = 5.2 \times 10^{-11}$ m^2)

Dynamics of advective oxygen transport at a mound

Because in the natural environment flow conditions can vary, we were interested in the time scale of advective oxygen supply to a certain sediment depth after a change of flow velocity. Two electrodes were positioned at fixed sediment depths of 3 and 20 mm at the upstream foot of the mound ($x = 0$) to follow the oxygen concentration at these particular depths under varying flow conditions (Fig. 10). After equilibration of the oxygen flux at a flow velocity of 10 cm s^{-1} the flume motor was switched off and the decrease of oxygen concentration in the respective sediment depths were recorded by a data logger at intervals of 1 s. As a steady state of oxygen concentration was reached, the motor was switched on again. At the beginning of the experiment the oxygen concentrations at 3 and 20 mm were 210 and 115 µmol oxygen l^{-1} respectively; these values corresponded to the oxygen profile measured at this location ($x = 0$) at a current speed of 10 cm s^{-1} (Fig. 5). As the flow was turned off, the oxygen value in 20 mm sediment depth declined to zero within 2 h. In the upper sediment layer, in 3 mm depth, oxygen decreased to a concentration of 10 to 15 µmol l^{-1}, which was maintained over a period of 8 h under no-flow conditions. As the water flow was started again, this oxygen sensor's signal increased almost instantaneously (within 30 s). The initial value of 210 µmol oxygen l^{-1} was stable after 50 min and stayed constant. At the depth of 20 mm this effect was delayed, after 1 h 48 min an increase of oxygen was measured. It took another 1 h 20 min until a concentration of ca 90 to 100 µmol l^{-1} was reached.

The oxygen uptake or respiration (R) in the respective depth could be estimated from the initial (after 30 s) decrease (∂C) of oxygen with time (∂t): $R = \partial C/\partial t$.

In 3 mm the respiration was 7×10^{-6} µmol O_2 cm^{-3} s^{-1} and slightly higher than the oxygen uptake of 5×10^{-6} µmol O_2 cm^{-3} s^{-1} in 20 mm sediment depth.

DISCUSSION

Advective transport of oxygen

Diffusive oxygen flux across the sediment-water interface is driven by a concentration gradient be-

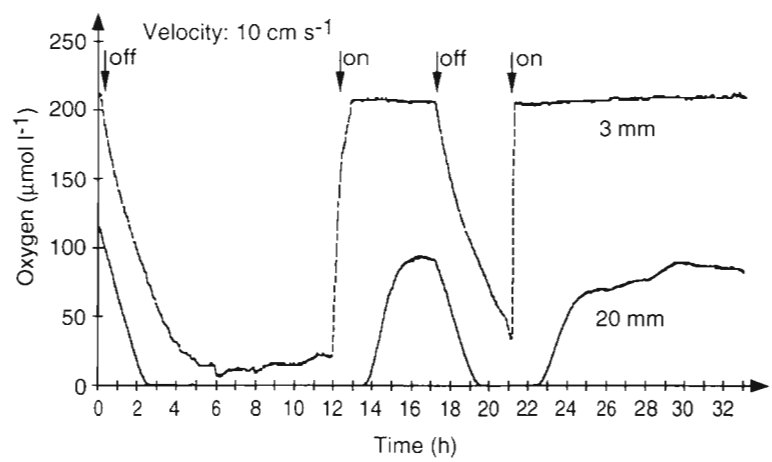

Fig. 10. Oxygen concentrations were continuously measured in 3 mm and 20 mm sediment depth for 32 h at the same position ($x = 0$) at the upstream foot of the *Callianassa truncata* sediment mound. The initial current velocity of 10 cm s^{-1} was turned on and off twice. Time resolution was 1 s

tween the overlying water and the pore water. It is dependent on the oxygen concentration in the supernatant water (Rasmussen & Jørgensen 1992) and the diffusion coefficient of oxygen in the water and the sediment. The oxygen penetration depth depends on the oxygen uptake of the sediment (Reimers & Smith 1986, Revsbech & Jørgensen 1986) and thus on the organic content. As the O_2 concentration decreases with depth due to biological and chemical consumption (Crank 1983) the microscale measured profiles may show a change in the gradient, allowing the calculation of the oxygen uptake in a defined zone (Crank 1983, Nielsen et al. 1990).

The oxygen gradients we measured in the permeable sand, underneath a smooth surface, corresponded to the oxygen profiles measured in other coastal regions. The penetration depth was ca 4 mm and a typical curve of nearly parabolic shape indicated a steep decline of oxygen with depth. At a smooth surface the change of the boundary layer flow velocity did not significantly affect the oxygen transport across the interface (Fig. 4), although minor changes were possibly not detected due to the error of sediment surface detection. The penetration depth of oxygen under stagnant conditions was in the same range of ca 4 mm. In early investigations, Fenchel (1969) also demonstrated that a moderate current of 8 cm s^{-1} above natural sands of increasing permeability did not result in advective pore water movements below 4 mm sediment depth.

In high-resolution measurements, Jørgensen & Des Marais (1990) showed that oxygen penetration increased 3-fold (from 0.5 mm to 1.5 mm) in a bacterial mat as the flow speed was increased by a factor of 25 (0.3 cm s^{-1} to 7.7 cm s^{-1}). Their explanation was a reduced thickness of the diffusive boundary layer (DBL). The DBL is a thin layer of water, typically only 0.2 to 1 mm thick (Boudreau & Guinasso 1982, Jørgensen & Revsbech 1985, Gundersen & Jørgensen 1990), covering the sediment surface. Within the DBL the viscous forces exceed the turbulent, and molecular diffusion is the dominant transport mechanism. Oxygen decreases linearly as the sediment surface is approached. With increasing current velocity the thickness of the DBL decreases and as a result oxygen concentration directly at the interface is higher and the solute penetrates deeper into the sediment. In our experiments, in the sandy sediment (median diameter 350 µm) from the Mediterranean Sea, the measured profiles do not show the formation of a DBL. One explanation might be the insufficient resolution of the measurements. We assume that the formation of this layer was most likely affected by the sediment surface roughness. Obstacles protruding more than half of the DBL thickness into the overlying water can influence the formation of this laminar layer (Vogel 1983). The absence of a DBL might indicate some advective flow in the upper few mm of the sediment even in the case of a 'smooth' surface. The average oxygen penetration under stagnant conditions was 4.8 mm (n = 6), so that we assume that advective transport rate at a smooth surface of the sandy sediment was comparable to the diffusive flux of oxygen across the sediment-water interface.

In contrast, hydrodynamic forces determined the interfacial solute transport at the roughness element in the permeable sediment. In the vicinity of the small biogenic mound (1 cm high) the small-scale flow field was altered (Fig. 3) and as a consequence pressure differences were generated. Within the high pressure fields, not only did oxygen reach down to deeper layers but the profiles also showed a characteristic change in shape (Fig. 5). High concentrations persisted up to 20 mm deep into the sediment. The curve of the profile indicates that the oxygen supply is higher than the concurrent uptake at the respective sediment depths. The deep oxygen penetration cannot be explained by diffusional pathways but is due to advection. Consequently, the O_2 uptake cannot be calculated from the profile's shape, as is possible for diffusive oxygen gradients using Fick's first law of diffusion ($J = -D_s \cdot \partial C/\partial x$, where J is the diffusion flux, D_s the apparent diffusion coefficient in the substrate and $\partial C/\partial x$ is the slope of the concentration profile at depth x).

In contrast to dyes, used as conservative tracers in experiments designed to show advective transport (Huettel & Gust 1992), oxygen is one of the most reactive chemical species. While being transported it is also consumed in biological and chemical processes, thus the measured profiles describe a dynamic balance between oxygen supply and consumption in the specific depth. In dye experiments under similar flow conditions and a structure of comparable size, the solute reached down to more than 5 cm sediment depth (Huettel & Gust 1992).

The depth distribution of oxygen at the obstacle was a function of flow velocity. Penetration depth and thus the sediment volume oxygenated were greatest at the highest flow velocity used in our experiments (10 cm s^{-1}), a current speed commonly observed in the natural environment. A total volume of ca 98 cm^3 of sediment was calculated to be oxic next to this mound of 10 mm height. This compares to 20 cm^3 of sediment supplied with oxygen by diffusion, considering an equivalent area (51 cm^2) of a smooth sediment surface. Thus the oxic volume increased locally by a factor of 4.8. This means a significant increase of oxygen availability for aerobic respiration and oxygen-dependent chemical reactions. In the natural environment the sediment volume supplied with oxygen by advection is related to the density of biogenic structures in a given area. At the observed natural density of 120 callianassid mounds per m^2, a 3.3-fold increase of oxygenated

sediment compared to a smooth surface could be expected, under the assumption of a uniform shape of mounds (10 mm height) and a steady unidirectional flow of 10 cm s^{-1}. Concerning the dimensions of the structures, we showed a minimum effect, as the height of the mound used in the experiment was relatively small compared to the average height (4 cm) of structures at the study site. Oxic zones of greater dimensions probably occur in the field. Furthermore, we considered only the conspicuous mounds for our estimations, but besides other irregularities of the interface, twice the number of funnel-shaped depressions (3 cm deep) than mounds characterised the sediment surface at the Mediterranean study site (240 m^{-2}). Here boundary layer flows are altered in a similar way and generate pressure differences that add to the importance of advective oxygen transport (Huettel & Gust 1992). In the investigated area the sediment surface topography was mainly characterised by the burrowing activity of the thalassinid shrimp. In other coastal areas sedimentological structures such as ripples may influence the boundary layer flow and thus contribute to an enhanced exchange of dissolved and particulate matter between the water column and the sea bed (Huettel & Gust 1992, Huettel et al. 1996). On the other hand, wave-induced bottom stress has to be considered when evaluating sediment-water exchange processes in coastal areas. Frequent resuspension of the upper sediment layer might have a greater influence on oxygenation effects in some areas than biologically mediated oxygen transport. Detailed information on the boundary layer flow conditions as well as on abundances, shapes and dimensions of biogenic or geological structures are necessary to assess the magnitude of advective interfacial solute exchange.

Physical sediment properties, such as grain size composition and porosity, determine the permeability of a seabed. Permeability is a crucial factor for solute transport in sediments and strongly depends on the actual size of sand grains (in contrast to porosity) and on the degree of sediment sorting. The North Sea sediment had a similar porosity and amount of organic content as the Giglio sediment, but was characterised by a smaller grain size and thus a lower permeability. In this less-permeable sediment there was a 2-fold increase in oxygen penetration at the upstream side of the mound at a current velocity of 10 cm s^{-1}, suggesting an advective solute transport. Huettel & Gust (1992) stated that in sediments with a permeability of $K > 2 \times 10^{-11}$ m^2 pressure gradients at the sediment surface would generate advective pore-water flow across the interface. The permeability of the North Sea sediment ($K = 5 \times 10^{-12}$ m^2) was lower than this value. It is also likely that a DBL existed at this finer-grained sediment surface. When the DBL was compressed, because of the higher current velocity, it allowed a deeper-reaching solute transport, which would explain the increased oxygen penetration depth.

Our experiments show that the effect of interstitial solute transport, produced by pressure gradients, is strongly dependent on the sediment permeability.

Variability of the oxic zone

In a permeable sediment with biogenic topography the oxic zone below the depth of diffusional transport is controlled by boundary flow velocities. Advective transport is initiated as soon as flowing water is deflected by the roughness element and is much faster than diffusional transport. In our experiment, after a change from stagnant water to a boundary layer flow of 10 cm s^{-1} (Fig. 10), it took ca 3 h until the sediment layer in 20 mm depth was continuously supplied with oxygen. For a comparison, the time required for a solute to overcome a distance by diffusional transport can be approximated by using the equation $t = z^2/2D$, derived from the definition of a 1-dimensional diffusion coefficient, where t is the time in s, z is the distance or sediment depth in cm and D the diffusion coefficient of a solute in water at a given salinity and temperature. The diffusion coefficient for oxygen in sea water with a salinity of 37‰ and a temperature of 19°C would be $D = 1.9214 \times 10^{-5}$ cm^2 s^{-1}.

According to this calculation it would take 29 h for an oxygen molecule to overcome a distance of 20 mm in sea water by molecular diffusion. In the sediment the time required would be prolonged (ca 3-fold) due to the porosity and tortuosity effects (Berner 1980, Iversen & Jørgensen 1993).

Underneath an irregular surface and within a few centimetres' sediment depth the availability of oxygen can change rapidly with varying flow conditions. Furthermore, the topography of the sea floor is not permanent but varies with faunal activity, which is often seasonal because it is stimulated by the input of organic carbon from the water column and reflects generation cycles. Most biogenic structures are not stable but change in size and are erased by strong currents. In turn, high boundary-layer flow velocities not only render the sediment more permeable but can generate ripples that produce similar advective transport processes (Thibodeaux & Boyle 1987).

Another important aspect of topography-induced solute transport is the upwelling of reduced pore water due to the low pressure field above a mound or ripple. The isopleths (Fig. 6) show that the oxic zones, upstream and downstream of the mound, are separated by an anoxic region underneath the mound, where reduced solutes reach the sediment surface.

Pore water from as deep as 20 cm can be transported to the sediment surface by this suction effect (Huettel & Gust 1992). The presence of this oxygen-free zone next to oxic environments further complicates the zonation pattern and creates horizontal gradients of oxygen concentration within the upper sediment layer The oxygen distribution in natural environments is heterogeneous and highly variable, thus many factors have to be considered when estimating solute exchange rates.

Implications for the sedimentary environment

Advective oxygen transport can play an important role in the ecology of coastal sediments. Many coastal areas and a large part of the continental shelf (40%) are covered by permeable sediments that are exposed to boundary layer flows and are populated by infaunal organisms or are characterised by ripples. Thus advective transport processes take place that can expand the oxic sediment volume far beyond the zone supplied by diffusion. The increase of free oxygen available for aerobic respiration enhances the mineralisation of organic matter and the subsequent release of regenerated nutrients can be of importance for the ambient environment. Reduced substances are oxidised within the flushed regions or locally at the sediment interface where anoxic pore water is transported upward due to the low pressure on top of elevations. Parallel to the advective solute transport, organic particles are transported into the interstices of the permeable sea bed (Huettel et al. 1996). The co-occurring input of oxygen and organic matter further promotes microbial carbon oxidation and accelerates remineralisation processes within the upper sediment. The oxygen used in surplus during advective transport compared to diffusional supply for respiration and chemical or biological oxidation must also be reflected in the total oxygen uptake of the sediment (Forster et al. unpubl.) Next to food availability, oxygen is the predominant factor determining the habitat conditions for aerobic micro- and meiofauna. The existence of anaerobic life forms is also not possible in isolation from oxic regions, as the essential chemical energy is provided by the processes that take place in the oxic zones. Anaerobic life has therefore been found to be most abundant in the vicinity of aerobic habitats (Fenchel & Finlay 1995). In sandy sediments the numbers of protozoans are highest at the transition zone from anoxic to oxic conditions (Giere 1993). This is also the region where bacterial activity is often found to be highest (Fenchel & Blackburn 1979). Many protozoans are microaerophilic, but are sensitive to higher O_2 concentrations, which can be toxic for them. The results of this investigation show that due to topography-induced flow effects the oxic-anoxic transition becomes 3-dimensional, offering an enlarged habitat for gradient organisms. We showed that this region is also characterised by a high spatial and temporal variability. This implies that the organisms have to react with high mobility to meet their metabolic needs or to escape unfavourable conditions, if they are not able to tolerate the changing conditions (Alve & Bernhard 1995). Classification of micro-organisms according to the sediment depth where they have been found is only reliable in combination with the exact description of chemical gradients. Foraminifera, for example, have been observed in 'anoxic' habitats, but species with anaerobic metabolism probably do not exist (Bernhard 1989, Bernhard & Reimers 1991). An explanation would be the supply of oxygen to deeper sediment layers. The observed downward migration in Foraminifera as a response to flow (Palmer & Molloy 1986) might be an indication for this.

The presence of biogenic structures at a permeable sea floor exposed to moderate boundary layer flows induces a high spatial and temporal variability of oxygen concentration within the upper layer of the sediment and may also affect the exchange of other dissolved substances between the water column and the sediment. The advective supply of oxygen to a permeable seabed far exceeds diffusional transport and may essentially affect mineralisation processes within the sediment and the distribution of benthic meiofauna and micro-organisms.

Acknowledgements. We thank Anja Eggers, Gabriele Eickert and Anni Glud of the microsensor laboratory at our institute for the construction of oxygen microelectrodes. The study was supported by the Max Planck Society.

LITERATURE CITED

Aller RC (1982) The effects of macrobenthos on chemical properties of marine sediment and overlying water. In: McCall PL, Tevesz MJS (eds) Animal-sediment relations (2): topics in geobiology. Plenum Press, New York, p 53–96

Aller RC (1983) The importance of the diffusion permeability of animal burrow linings in determining marine sediment chemistry. J Mar Res 41:299–322

Alve E, Bernhard JM (1995) Vertical migratory response of benthic Foraminifera to controlled oxygen concentrations in an experimental mesocosm. Mar Ecol Prog Ser 116: 137–151

Andersen FO, Helder W (1987) Comparison of oxygen microgradients, oxygen flux rates and electron transport system activity in coastal marine sediments. Mar Ecol Prog Ser 37: 259–264

Berner RA (1980) Early diagenesis — a theoretical approach. Princeton University Press, Princeton, NJ

Bernhard JM (1989) The distribution of benthic foraminifera with respect to oxygen concentration and organic carbon levels in shallow-water Antarctic sediments Limnol Oceanogr 34:1131–1141

Bernhard JM, Reimers CE (1991) Benthic foraminiferal popu-

lations related to anoxia Santa Barbara Basin. Biogeochemistry 15:127–149
Berninger UG, Epstein S (1995) Vertical distribution of benthic ciliates in response to the oxygen concentration in an intertidal North Sea sediment. Aquat Microb Ecol 9: 229–236
Blackburn TH (1987) Microbial foodwebs in sediments. In: Sleigh MA (ed) Microbes in the sea. Wiley, Chichester, p 39–57
Boudreau BP, Guinasso NL (1982) The influence of a diffusive sublayer on accretion, dissolution and diagenesis of the sea floor. In: Fanning KA, Mannheim FT (eds) The dynamic environment of the ocean floor. Lexington Books, Lexington, MA, p 115–145
Crank J (1983) The mathematics of diffusion. Clarendon Press, Oxford
Dworschak PC (1983) The biology of *Upogebia pusilla* (Petagna) (Decapoda, Thalassinidea) I. The burrows. Mar Ecol 4:19–43
Fenchel T (1969) The ecology of marine microbenthos IV Structure and function of the benthic ecosystem, its chemical and physical factors and the microfauna communities with special reference to the ciliated protozoa. Ophelia 6: 1–182
Fenchel T, Blackburn TH (1979) Bacteria and mineral cycling. Academic Press, London
Fenchel T, Finlay BJ (1995) Ecology and evolution in anoxic worlds. Oxford University Press, Oxford
Forster S, Graf G (1992) Continuously measured changes in the redox potential influenced by oxygen penetrating from burrows of *Callianassa subterranea*. Hydrobiologia 235/236:527–532
Forster S, Graf G (1995) Impact of irrigation on oxygen flux into the sediment: intermittent pumping by *Callianassa subterranea* and 'piston-pumping' by *Lanice conchilega*. Mar Biol 123:335–346
Giere O (1993) Meiobenthology: the microscopic fauna in aquatic sediments. Springer-Verlag, Berlin
Griffis RB, Suchanek TH (1991) A model of burrow architecture and trophic modes in thalassinidean shrimp (Decapoda: Thalassinidea). Mar Ecol Prog Ser 79:171–183
Gundersen JK, Jørgensen BB (1990) Microstructure of diffusive boundary layers and the oxygen uptake of the sea floor Nature 345:604–607
Huettel M (1990) Influence of the lugworm *Arenicola marina* on porewater nutrient profiles of sand flat sediments. Mar Ecol Prog Ser 89:253–267
Huettel M, Gust G (1992) Impact of bioroughness on interfacial solute exchange in permeable sediments. Mar Ecol Prog Ser 62:241–248
Huettel M, Ziebis W, Forster S (1996) Flow-induced uptake of particulate matter in permeable sediments. Limnol Oceanogr 41:309–322
Hylleberg J, Henriksen K (1980) The central role of bioturbation in sediment mineralisation and element recycling. Ophelia 1:1–16
Iversen N, Jørgensen BB (1993) Diffusion coefficient and methane in marine sediments. Geochim Cosmochim Acta 75:571–578
Jørgensen BB, Des Marais DJ (1990) The diffusive boundary layer of sediments: oxygen microgradients over a microbial mat. Limnol Oceanogr 35(6):1343–1355
Jørgensen BB, Revsbech NP (1985) Diffusive boundary layers and the oxygen uptake of sediments and detritus. Limnol Oceanogr 30(1):111–122
Jørgensen BB, Revsbech NP (1989) Oxygen uptake, bacterial distribution and carbon-nitrogen-sulfur cycling from the Baltic Sea - North Sea transition. Ophelia 31(1):29–49
Kristensen E (1985) Oxygen and inorganic nitrogen exchange in a *Nereis virens* (Polychaeta) bioturbated sediment-water system. J Coast Res 1:109–116
LaBarbera M, Vogel S (1976) An inexpensive thermistor flowmeter for aquatic biology. Limnol Oceanogr 21:750–756
Mackin JK, Swider KT (1989) Organic matter decomposition pathways and oxygen consumption in coastal marine sediments. J Mar Res 47:681–716
Malan DE, McLachlan A (1991) *In situ* benthic oxygen fluxes in a nearshore coastal marine system: a new approach to quantify the effect of wave action. Mar Ecol Prog Ser 73: 69–81
Means RE, Parcher JV (1964) Physical proportion of soils. Constable, London
Meyer-Reil L, Faubel A, Graf G, Thiel H (1987) Aspects of a benthic community structure. In: Rumohr J, Walger E, Zeitschel B (eds) Seawater-sediment interactions in coastal waters — an interdisciplinary approach. Springer, Heidelberg, p 69–110
Nielsen LP, Christensen PB, Revsbech NP, Sørensen J (1990) Denitrification and oxygen respiration in biofilms studied with a microsensor for nitrous oxide and oxygen. Microb Ecol 19:63–72
Palmer MA, Molloy RM (1986) Water flow and the vertical distribution of meiofauna: a flume experiment. Estuaries 9: 225–228
Rasmussen H, Jørgensen BB (1992) Microelectrode studies of seasonal oxygen uptake in a coastal sediment: role of molecular diffusion. Mar Ecol Prog Ser 81:289–303
Reimers C, Smith KL Jr (1986) Reconciling measured and predicted fluxes of oxygen across the deep sea sediment-water interface. Limnol Oceanogr 31:305–318
Revsbech NP (1989) An oxygen microsensor with a guard cathode. Limnol Oceanogr 34:474–478
Revsbech NP, Jørgensen BB (1986) Microelectrodes: their use in microbial ecology. Adv Microb Ecol 9:293–352
Revsbech NP, Jørgensen BB, Blackburn TH (1980) Oxygen in the sea bottom measured with a microelectrode. Science 207:1355–1356
Riedl R, Huang N, Machan R (1972) The subtidal pump, a mechanism of intertidal water exchange by wave action. Mar Biol 13:210–221
Schlichting H (1987) Boundary layer theory, 7th edn. McGraw-Hill, New York
Thibodeaux LJ, Boyle JD (1987) Bed-form generated convective transport in bottom sediment. Nature 325(6102): 341–343
Vogel S (1983) Life in moving fluids. Princeton University Press, Princeton, NJ
Yager PL, Nowell ARM, Jumars PA (1993) Enhanced deposition to pits: a local food source for benthos. J Mar Res 51 209–236

This article was submitted to the editor

Manuscript first received: February 28, 1996
Revised version accepted: May 21, 1996